Inorganic Chemistry

Article

pubs.acs.org/IC

Probing the Steric and Electronic Characteristics of a New Bis-Pyrrolide Pincer Ligand

Nobuyuki Komine, René W. Buell, Chun-Hsing Chen, Alice K. Hui, Maren Pink, and Kenneth G. Caulton*

Department of Chemistry, Indiana University, 800 East Kirkwood Avenue, Bloomington, Indiana 47405, United States

Supporting Information

ABSTRACT: A new pincer ligand is synthesized to be dianionic, with the potential to be redox active. It has pyrrole rings attached to both ortho sites of a pyridine, as the linking element. This H_2L can be doubly deprotonated and then used to replace two chloride ligands in $MCl_2(NCPh)_2$, to form LM(NCPh) for M = Pd, Pt. The acid form H_2L reacts with $ZnEt_2$ with elimination of only 1 mol of ethane to yield (HL)ZnEt, a three-coordinate species with one pendant pyrrole NH functionality. This molecule binds the Lewis base *p*-dimethylaminopyridine (DMAP) to give first a simple 1:1 adduct that eliminates ethane on heating to form four-coordinate LZn(DMAP), which has an unusual structure due to the strong preference of the pincer ligand to bind in a *mer* (planar) geometry. A molecule with two HL^- ligands each bonded in a bidentate manner to $FeCl_2$ is synthesized and shown to contain four-coordinate iron with a flattened-tetrahedral structure. The electrochemistry of LM(NCPh) and (L)Zn(DMAP) shows three oxidation processes, which is interpreted to involve at least two oxidations of the pyrrolide arms.

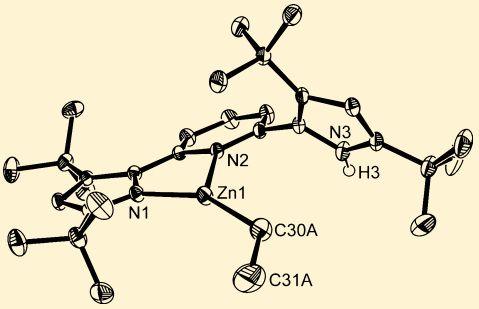

INTRODUCTION

As a class, pincer ligands have seen explosive growth,[1] and their advantages are increasingly understood.[2−10] Their *mer* stereochemistry leaves coplanar coordination sites; this is in contrast to tris(pyrazolyl)borates or cyclopentadienyl ligands with their obligatory *fac* geometry and allows pincer-induced stereochemical control, including imposed chirality. As working functionalities, pincers are modular and carry a number of sites for NMR evaluation, for solubilizing the complex (even in noninteracting solvents), and for enhancing their capacity to be analyzed in the gas phase (mass spectrometry). Their tridentate character suppresses degradative ligand loss and even discourages "arm off" mechanistic steps (a "self-repairing" $\kappa^2 \rightarrow \kappa^3$ arm reattachment is entropically favored by ∼11 kcal/mol at room temperature).

In constructing a pincer ligand which is potentially redox active, we have chosen to include a pyrrolide.[11−13] As a substituent on an aryl (pyridine) ring, pyrrolide gives (**1** in Scheme 1) amide nitrogen character to the pyridine partner, via conjugation between the two rings. This *ring* is an electron-donating *substituent* by its Hammett parameters and is certainly also a π donor to a metal due to its amide character. This latter feature will certainly be diminished, in comparison to a dialkylamide, by virtue of involvement of the amide lone pair in the aromaticity of the pyrrole (smaller resonance energy in comparison to that of benzene).[11] Pyrroles themselves are powerful ancillaries to increasing the reducing power of metals, promoting reduction of N_2, CO_2, and other poor ligands.[14−18] By coupling the pyrrolide ligand to a reducible ligand, pyridyl, (whose π^* orbitals permit reduction), we create a push/pull ligand of enhanced potential redox character in comparison to that of neutral bipyridyl. The push/pull character makes the pyridylpyrrolide capable of being reduced or of being oxidized, hence a useful ancillary to metal complexes under *either* reducing or oxidizing conditions. We report here the chemistry of a pincer ligand, H_2L in Scheme 1, which includes these functionalities. Since the two pyrroles employed here carry two tBu groups, this new ligand should be especially electron rich and subject to ready oxidation.

Characterization of 2,6-bis(R)pyridine pincer complexes (R = indolyl, azaindolyl) of several divalent metals have been reported, for their optical properties, and all have conventional κ^3 pincer connectivity.[19,20]

We illustrate different methods for attaching this pincer ligand to metals, the redox activity of the resulting complexes, and the ability to break the 2-fold symmetry of this pincer by synthesis of complexes with inequivalent arms. We find a

Scheme 1

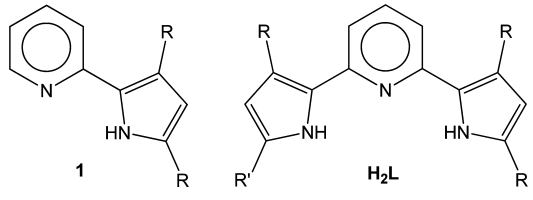

Received: August 19, 2013
Published: January 10, 2014

ACS Publications © 2014 American Chemical Society

dx.doi.org/10.1021/ic402120r | *Inorg. Chem.* 2014, 53, 1361−1369

Scheme 2

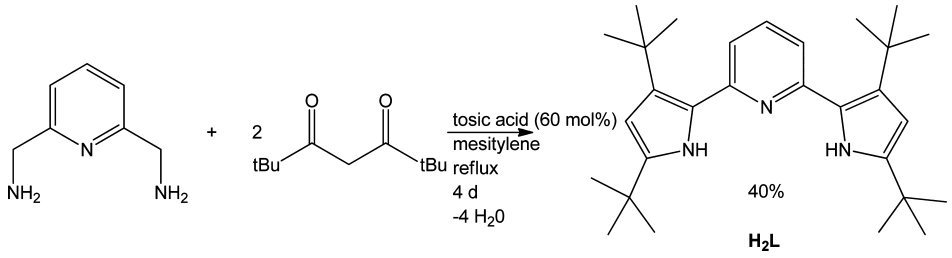

surprising ability of one acidic pyrrole NH functionality to coexist with a metal alkyl, and we attempt to utilize the general phenomenon of our pendant pyrrole NH functionality to participate actively by interaction with substrate.

RESULTS

Ligand Synthesis and Its d^8 Complexes. The ligand was synthesized according to the route in Scheme 2, first installing the amino substituents on the pyridyl ortho positioned CH_2 arms and then ring closing twice via the procedure of McNeill.[21] Spectroscopic characteristics are unexceptional. The ligand free base is soluble not only in the polar solvents acetone and methanol but also in benzene and pentane. Single crystals, grown by slow evaporation from acetonitrile, were shown (Figure 1) by X-ray diffraction to adopt a conformation

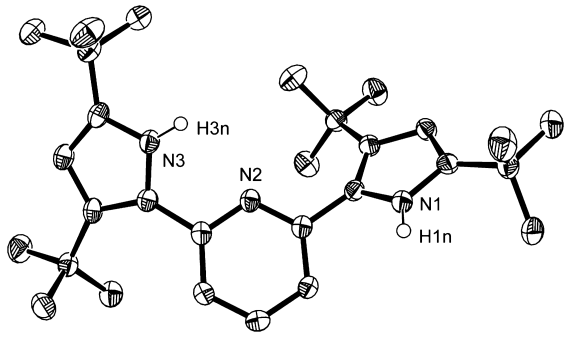

Figure 1. ORTEP drawing of the non-hydrogen atoms of H_2L showing selected atom labeling. Unlabeled atoms are carbons. The acetonitrile guest molecule in the asymmetric unit is not shown but is responsible for the outward orientation of the N1−H1n bond.

with the pyrroles not directed exclusively inward, but one pyrrole NH bond is directed outward (NCCN dihedral angle 137.5°) in order to hydrogen bond to a lattice guest acetonitrile nitrogen (N−N = 3.124(4) Å). The second pyrrole has an NCCN dihedral angle of 26.1°; both of these pyrrole ring rotations diminish steric interference between the close ^{t}Bu group and the pyridyl ring.

This free base H_2L is readily deprotonated with KH in THF to yield a free-flowing solid K_2L salt, for use in installing the ligand on transition-metal halides. Reaction of K_2L with $MCl_2(NCPh)_2$ for M = Pd, Pt gives products, following filtration and vacuum removal of volatiles, whose NMR spectra are consistent with C_{2v} symmetry, with intensities consistent with the formula LM(NCPh). A single-crystal X-ray structure determination of LPt(NCPh) (Figure 2) shows the molecule to have a planar structure with benzonitrile nitrogen trans to the pyridyl nitrogen. Nitrile nitrogen has a shorter bond length to Pt than the pyrrolides, with the pyridyl nitrogen shortest of all. The pincer bite angle constraint leaves the interpyrrolide angle

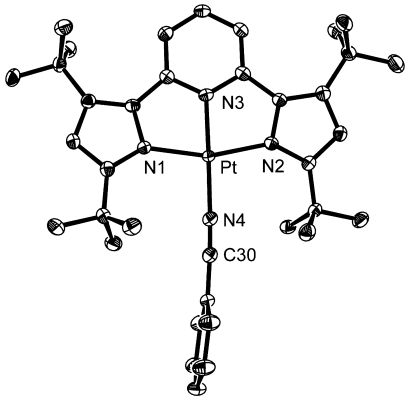

Figure 2. ORTEP view (50% probability) of the non-hydrogen atoms of LPt(NCPh), showing selected atom labeling. Unlabeled atoms are carbon. Selected structural parameters (distances in Å and angles in deg): Pt1−N1, 2.061(2); Pt1−N2, 2.053(2); Pt1−N3, 1.950(2); Pt1−N4, 1.982(3); N4−C30, 1.143(4); N1−Pt1−N2, 161.08(10); N1−Pt1−N3, 80.78(10); N2−Pt1−N3, 80.34(10); N1−Pt1−N4, 98.57(10); N2−Pt1−N4, 100.34(10); N3−Pt1−N4, 78.04(10); Pt1−N4−C30, 178.1(3).

N1−Pt−N2 at 161.08(10)°. The dihedral angles NCCN involving pyrrolide and pyridyl in LPt(NCPh) are 2.1 and 4.1°, indicating that the rings are conventionally eclipsed and coplanar. The steric impact of the ^{t}Bu groups is seen in the benzonitrile conformation, which is perpendicular to the coordination plane to maximize distances to the ^{t}Bu groups.

The two LM(NCPh) complexes show rich electron transfer reactivity. Cyclic voltammograms were run in *o*-difluorobenzene with 0.3 M $[N(n\text{-}Bu)_4][PF_6]$ at 100 mV s^{-1}, and all are referenced to Fc/Fc^+ as 0.0 V. Both molecules show (Figure 3) three oxidations, with the first (very low potential of about +0.13 V) and third being reversible (about +1.10 V). The potentials for these are metal independent to within 0.05 V, which leads to assigning these to ligand-based oxidations, and are primarily from the electron-rich pyrroles.[22] Since, for a given metal, these first and third potentials are very different (by ∼1 V), this means that the two pyrrolides communicate strongly: the single oxidation occurs delocalized over both pyrrolides. The second oxidation is reversible only for Pt. Down to −2.5 V, the Pt compound is not electroactive, but the Pd example shows a reversible reduction with $E_{1/2}$ = −1.48 V; this different reductive behavior is consistent with the generally easier reduction of 4d than 5d metal, hence supporting an assignment of the reduction as metal based.

For comparison, CV of H_2L itself under identical conditions shows no reduction and shows three irreversible oxidations, at E_{pa} = 0.55, 1.07, and 1.33 V (see the Supporting Information).

Carbonylation. We were interested in obtaining a CO stretching frequency to compare the donor power of bis-

dx.doi.org/10.1021/ic402120r | Inorg. Chem. 2014, 53, 1361−1369

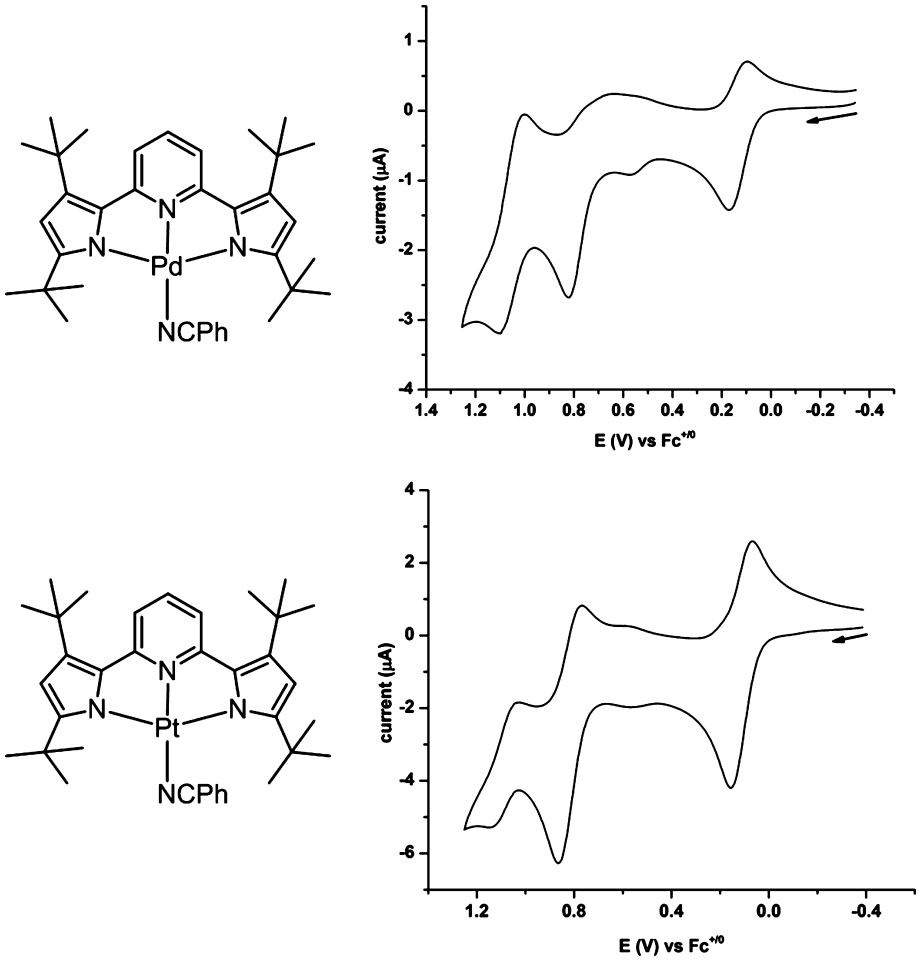

Figure 3. Cyclic voltammograms of LPd(NCPh) (top) and LPt(NCPh) (bottom) in *o*-$C_6H_4F_2$.

pyrrolylpyridine pincer to that of other ligand sets. Reaction of LPd(NCPh) with 1 atm of CO in CH_2Cl_2 yields LPd(CO). The CO stretching frequency of this product is 2197 cm^{-1}. Curiously, this is significantly higher than the value 2135 cm^{-1} for $PtCl_2$(pyridine)(CO),[23] which would place pyrrolide as a weaker donor than chloride. While the generally poor π donor ability of Pt(II) leaves all its carbonyl complexes at relatively high frequency, this ranking still shows that the Nπ lone pair of pyrrolide is significantly tied up in pyrrole aromaticity.

Zinc. Zinc coordination chemistry defies generalization.[24−29] Coordination numbers range from 3 to 6, although any coordination number higher than 4 violates the 18-electron rule. For example, there is firm structural confirmation that the water complex of zinc contains six water molecules coordinated in an octahedral structure. While conventional thinking indicates that four-coordinate, 18-valence-electron d^{10} divalent zinc should have a tetrahedral structure, there are violations. There are a huge number of zinc porphyrin complexes,[25,26] all of which have four-coordinate planar zinc with no axial ligation. Three-coordinate examples[28] generally require steric bulk to achieve such a level of unsaturation, and the resulting species are planar. However, a C_2-symmetric tridentate ligand (i.e., a pincer) is incompatible with the steric requirements of four-coordinate Zn(II).

Reaction of H_2L with $Zn(C_2H_5)_2$ (1:1 mole ratio) in benzene occurs to completion within 30 min at 25 °C to form a single yellow product which is soluble in benzene, pentane, and THF. The ^{1}H NMR spectrum shows that the two pyrrole arms of the ligand are inequivalent, as judged both by ring hydrogens and by observation of four ^{t}Bu chemical shifts. In addition, there is, at stoichiometric intensity, an A_2X_3 spin system evident indicative of one ethyl group per pincer ligand. The protonolysis of the ethyl groups thus proceeded only to the first step, leaving one pyrrole NH proton, evident at 6.94 ppm in a product of formula (HL)ZnEt. It is interesting that the NMR spectrum shows that there is no NH proton transfer (fast on the ^{1}H NMR time scale) to the deprotonated pyrrolide nitrogen, since that would make the two pincer arms time-averaged equivalent.

Single crystals grown by slow evaporation of a pentane solution were shown by single-crystal X-ray diffraction (Figure 4) to be of formula (HL)ZnEt, containing a monomeric species with three-coordinate zinc and singly deprotonated pincer ligand bound in a bidentate fashion to the metal. The three-coordinate geometry around zinc is approximately planar; the ethyl group is disordered over two sites so that N(pyrrolide)−Zn−C angles range from 146.6 to 151.89° while the N(pyridyl)−Zn−C angles range from 132.6 to 124.2°. The coordinated rings are nearly coplanar, with a NCCN dihedral angle of 6.6°. The NH-bearing pyrrole ring has a NCCN dihedral angle of 115.9°, and thus this ring presents its face to zinc or to the Zn−C bond. The NH bond is directed outward, away from zinc. The Zn−N(pyrrolide) distance is significantly *shorter* than the Zn−N(pyridyl) distance, 1.946 vs 2.074 Å, with the Zn−C distance intermediate at 1.970 Å; this is the opposite distance trend in comparison to LPt(NCPh). In spite of the

dx.doi.org/10.1021/ic402120r | *Inorg. Chem.* 2014, 53, 1361−1369

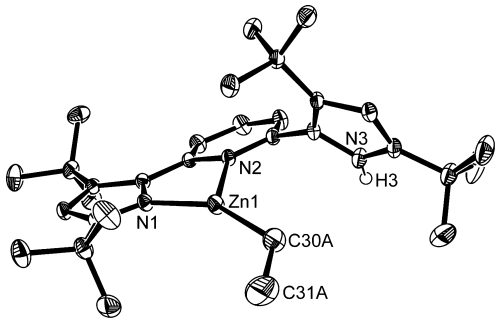

Figure 4. ORTEP view (50% probabilities) of the non-hydrogen atoms in the structure of (LH)Zn(C_2H_5), showing selected atom labeling; unlabeled atoms are carbons. Hydrogen on the pyrrole nitrogen is shown, for clarity. Selected structural parameters (distances in Å and angles in deg): Zn1−N1, 1.9462(14); Zn1−C30A, 1.969(8); Zn1−N2, 2.0740(15); N1−Zn1−C30A, 151.9(3); N1−Zn1−N2, 80.80(6); C30A−Zn1−N2, 124.1(3); C31A−C30A−Zn1, 119.6(13).

distortion of the ZnN_2C coordination geometry away from Y-shaped and toward T-shaped, there are no short inter- or intramolecular contacts with zinc shorter than van der Waals; the shortest are 2.5 Å to H and 3.0 Å to carbon.

Reactivity of (HL)ZnEt. Given our three-coordinate zinc ethyl complex (HL)ZnEt, we felt this might offer access to a T-shaped complex of zinc which could test the coordination geometry preferences and *limits*, as well as reactivity of such a Lewis acid. Efforts were therefore made to effect ethane elimination to form LZn. Heating (HL)ZnEt in benzene at 60 °C for up to 8 h showed no change, with recovery of reagent complex. We find this to be a remarkable coexistence of a metal alkyl with a nearby acidic proton. However, zinc and even aluminum alkyls are known to decrease dramatically the carbanionic character of the residual alkyl following proteolysis of the first alkyl,[30−35] although some examples of the reaction of HL with $ZnMe_2$ effect the complete loss of methyl groups, forming ZnL_2.[36]

We next attempted to probe the Lewis *acidity* of (HL)ZnEt, because of its low coordination number. This reacts in the time of mixing with *p*-dimethylaminopyridine (DMAP) to give a 1:1 adduct, established by integration of its ^{1}H NMR spectrum. This retains an NH proton and inequivalent pyrrole rings, as established by ^{1}H NMR. This (HL)ZnEt(DMAP) shows rapid exchange between free and coordinated DMAP in the presence of <1 equiv of additional DMAP, indicating rapid exchange of this Lewis base. Such exchange, by a dissociative mechanism, is thus the reason the diastereotopic inequivalence of the ethyl CH_2 protons is not resolved in the ^{1}H NMR spectrum of (HL)ZnEt(DMAP); the adduct is in rapid equilibrium with traces of (HL)ZnEt and free DMAP.

Synthesis of this DMAP adduct has a beneficial effect on ethane elimination. Simply heating a benzene solution of (HL)ZnEt(DMAP) to 50 °C gives conversion to (L)Zn-(DMAP). Proton NMR shows that this molecule has 2-fold symmetry of the two pyrrolide arms, shows no NH or ethyl proton signals, and retains the 1:1 stoichiometry of DMAP vs L. Of special interest is whether this is a monomer and whether such a monomer is planar or nonplanar. Attempts to see less than 2-fold symmetry of the DMAP in (L)Zn(DMAP) by ^{1}H NMR at −40 °C showed no decrease in symmetry of the two ortho or of the two meta DMAP protons.

Structure of (L)Zn(DMAP). Yellow crystals grown by slow evaporation of a dichloromethane solution were shown (Figure 5) by single-crystal X-ray diffraction to be four-coordinate monomers with a tridentate pincer ligand and DMAP

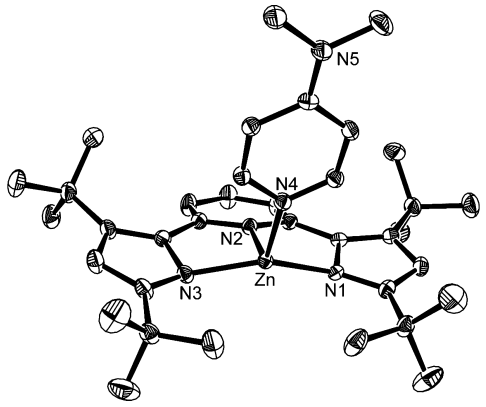

Figure 5. ORTEP view (50% probabilities) of the non-hydrogen atoms in the structure of (L)Zn(DMAP), showing selected atom labeling; unlabeled atoms are carbons. Selected structural parameters (distances in Å and angles in deg): N1−Zn1, 2.0036(15); N2−Zn1, 1.9886(14); N3−Zn1, 1.9883(15); N4−Zn1, 2.0162(15); N3−Zn1−N2, 81.85(6); N3−Zn1−N1, 146.80(6); N2−Zn1−N1 81.26(6); N3−Zn1−N4, 108.71(6); N2−Zn1−N4, 110.05(6); N1−Zn1−N4 103.89(6).

coordinated through the pyridine nitrogen. The molecule has idealized mirror symmetry, with equivalent pincer arms, in agreement with the ^{1}H NMR evidence. All four Zn−N distances fall in the narrow range 1.99−2.02 Å, but the constraint of the pincer ligand distorts the geometry so that zinc lies only slightly above the plane defined by the three pincer nitrogens and the DMAP nitrogen lies approximately perpendicular to that plane (the angle N2−Zn1−N4 is 110.05(6)°); the geometry is much closer to distorted tetrahedral than it is to planar, although a "see-saw" or cis-divacant octahedral description is the most valid. The main distortion from tetrahedral angles is the angle between the pyrrolides: N3−Zn1−N1 = 146.80(6)°. Symptomatic of the mismatch of pincer and zinc structural preferences, the pyrrole rings are not coplanar with the pyridine plane: the dihedral angles NCCN are 16.7 and 19.8°. Even more telling is the misdirection of the pyrrolyl nitrogen σ lone pair downward, away from the DMAP side of the pincer plane, and the pincer pyridyl nitrogen lone pair is oppositely misdirected (the C(para)−N−Zn angle is 172.5°). There is no evidence of steric clash between the ^{t}Bu groups adjacent to pyrrolyl nitrogen (Figure 6), but that region of the coordination sphere is too crowded to permit DMAP to coordinate there, trans to pincer pyridyl nitrogen. Nitrogen in the Me_2N substituent is planar, enhancing the electron richness of the DMAP pyridyl ring.

Cyclic Voltammetry of (L)Zn(DMAP). No reductions occurred out to −1.50 V. Three oxidation events are apparent (Figure 7) between 0 and 2 V. The first wave is quasi-reversible with E_{pa} at 0.018 V vs Fc/Fc^+. A control experiment shows that free DMAP in *o*-difluorobenzene has one irreversible oxidation at 0.568 V, suggesting that *one* oxidative process in Zn(L)-(DMAP) may be attributed to coordinated DMAP. The third wave is quasi-reversible with E_{pa} at 1.04 V vs Fc/Fc^+. This shows that the bis(pyrrolide)pyridyl ligand can be oxidized by up to two electrons below 1 V. The two pyrrolide arms communicate with each other, making the two oxidations

dx.doi.org/10.1021/ic402120r | Inorg. Chem. 2014, 53, 1361−1369

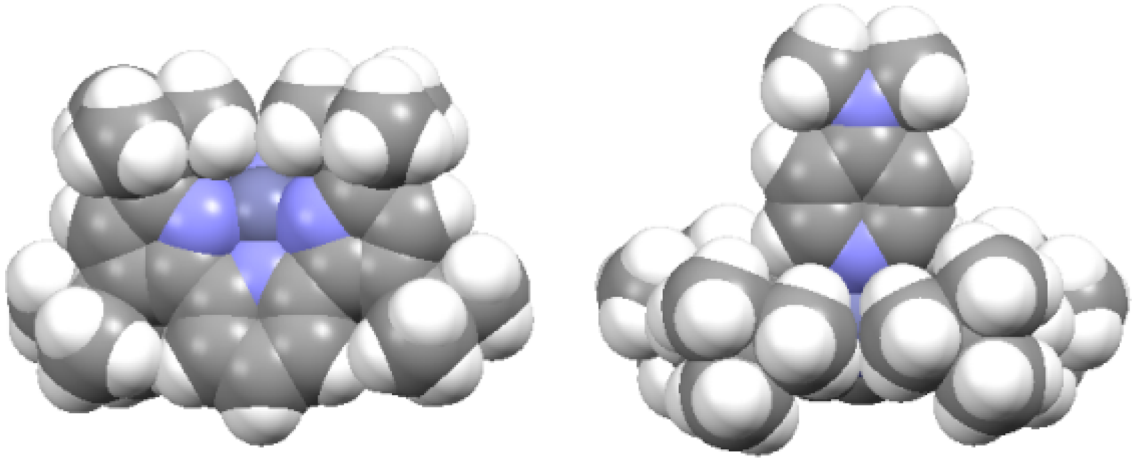

Figure 6. Space-filling models of (L)Zn(DMAP) (left) viewed trans to the DMAP, showing the open side of the coordination sphere, and (right) viewed trans to the pincer pyridyl nitrogen, to show close approach of the nearby ^{t}Bu groups, which forces the DMAP (vertical) out of the Zn/pincer plane.

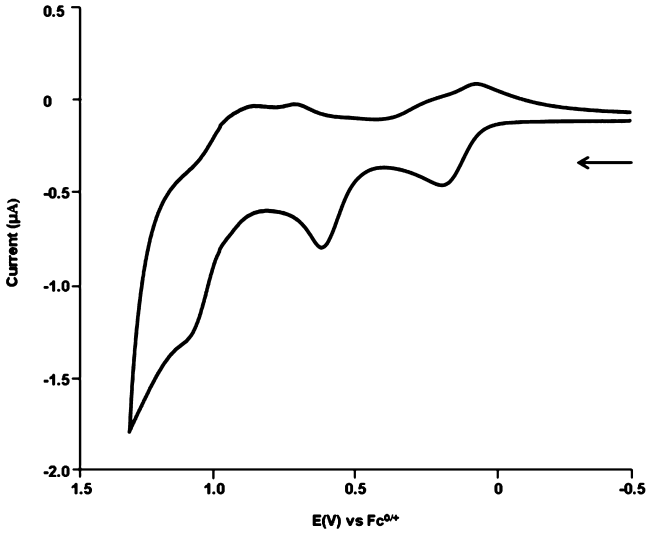

Figure 7. CV of (L)Zn(DMAP) in *o*-difluorobenzene. The scan rate is 100 mV/s, and the supporting electrolyte is 1.0 M [TBA]PF_6.

separate events at two different potentials. It is significant that three waves are also seen for the Pd and Pt complexes reported here (Figure 3) but that the oxidation potential of the zinc complex is less positive. This may be due to π/π repulsions[37] between the two pyrrolides and d^{10} zinc.

Mobilizing the NH Proton? In order to form a complex with zinc containing a dianionic κ^3-bis(pyrrolyl)pyridyl ligand, lithium bis(trimethylsilyl)amide was added to a benzene solution of (HL)Zn(Et) at room temperature in order to deprotonate the pyrrole nitrogen to form [Zn(L)(Et)]Li and bis(trimethylsilyl)amine. This reaction proceeds in the time of mixing, to give a new species which still contains an ethyl group, as judged by ^{1}H NMR spectroscopy. However, after volatiles (including $HN(SiMe_3)_2$) were removed by vacuum, the ethyl group was no longer present, as judged by the ^{1}H NMR spectrum (benzene solvent). Vacuum causes a change in product. The ethyl group could then be lost either as butane or as a 1:1 mixture of ethane and ethylene. The pyrrolide arms in this product have become chemically equivalent (on the NMR time scale), since only two ^{t}Bu peaks and three ligand backbone peaks are present. The ability of a base to form the new complex (which does not contain bound ethyl or trimethylsilyl amide/amine) suggests a product with the formula $[LiZn(L)]_n$. Attempts to crystallize the product have thus far been unsuccessful.

A key question is this: why does the pyrrole hydrogen not attack the zinc−ethyl bond in (LH)ZnEt? There is also a corollary question: why does binding Lewis base B to zinc facilitate that hydrogen transfer? The former question may hinge on the product, three-coordinate and T-shaped LZn being too high in energy to be reached in monomeric form. The latter question may require consideration of a non-least-motion mechanism for proton transfer. Instead of the reaction happening within an (LH)ZnEt(B) adduct, it may be (Scheme 3) that Lewis base B simply deprotonates the pyrrole nitrogen, and the resulting BH^+ then transfers its proton to the Zn−C bond in the $LZnEt^-$ anion, which may already have κ^3 pincer ligand connectivity and thus have a more polar Zn−C bond, hence being more acid sensitive; if proton transfer is concurrent with B/Zn binding, the transition state energy is kept low.

In summary, the importance of the Lewis base is not to lower the barrier to intramolecular proton transfer but instead to shuttle the proton from pyrrole nitrogen to the zinc−carbon bond. This clearly demands a Lewis base whose Brønsted basicity meets a narrow pK_a window: able to deprotonate

Scheme 3. Proposed Mechanism for Base-Assisted Elimination of Ethane from the Reaction Zn(HL)(Et) + Base

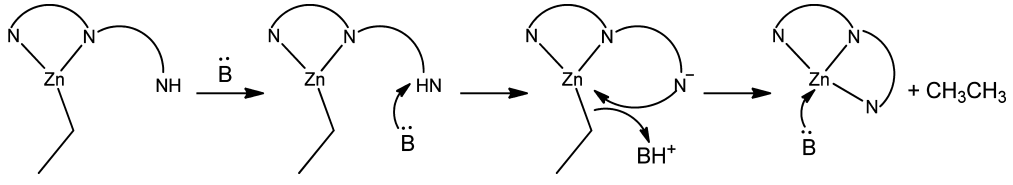

dx.doi.org/10.1021/ic402120r | Inorg. Chem. 2014, 53, 1361−1369

pyrrole nitrogen but still willing to surrender that proton to the zinc−carbon bond.

We investigated the hypothesis that it is not the adduct alone which facilitates protonolysis of the Zn−C bond by study of THF as the Lewis base; this has very poor Brønsted basicity. Adding 3 equiv of THF to a C_6D_6 solution of (LH)ZnEt shows adduct formation by a shift of all proton chemical shifts, including that of the pyrrole NH group. At 25 °C, there is no ethane release. The ^{1}H NMR spectrum also establishes that there is rapid exchange between free and coordinated THF, since the signals of both are coalesced. Heating of this solution to 60 °C for 24 h shows no change in the ^{1}H NMR spectrum, indicating that no proton transfer has occurred. Excess THF was employed in this experiment on the basis of the hypothesis that it is free base which transfers the proton from the pyrrole to the ethyl ligand. The basicity of THF is not strong enough to deprotonate the pyrrole nitrogen, and so this base is unsuitable for promoting loss of the ethyl moiety for produce Zn(L)-(base), in contrast to the case for DMAP. Also, the hypothesis that the presence of a base on Zn promotes ethane loss by sterically forcing the NH and ethyl groups closer together is contradicted by this THF adduct forming experiment.

Oxidation of (HL)Zn(Et) by 1 equiv of $AgBF_4$ or $^1/_2$ equiv of I_2 in benzene at room temperature results in degradation of the starting material into free ligand and several minor products. Removal of the pyrrole N−H proton in (HL)Zn(Et) by addition of KH was unsuccessful. H_2L itself undergoes no reaction with oxidants $AgBF_4$ and I_2 in THF at room temperature. Hence, attachment of the ring system to Zn(II) *increases* its tendency to oxidation (although this does lead to production of H_2L). This may originate from the anionic charge of the complexed ligand but may also be due to filled/filled repulsion[37] between the pyrrolide π system and the filled d orbitals.

Iron Complex with Two HL$^-$ Ligands. Given the persistence of an HL$^-$ ligand on zinc, we were interested in the generality of this form. Since we have characterized an iron complex with two *mono*pyrrolylpyridine ligands,[38] we chose to explore iron with our new pincer. Reaction of $FeCl_2$ with a 1:1 mixture of K_2L and H_2L in THF forms a single product, which we assign as Fe(HL)$_2$. This pentane-soluble molecule is most easily identified by detection of inequivalent arms in the ligand, particularly four strong 18H ^{t}Bu chemical shifts in benzene. The two ligands are thus symmetry related. Since the ring arms within a given pincer are inequivalent at 25 °C by ^{1}H NMR, there is no rapid proton transfer in this molecule, in spite of the close proximity of NH and pyrrolide N.

The product was established by single-crystal X-ray diffraction (Figure 8) as Fe(HL)$_2$, a complex with two singly deprotonated pincer ligands. The structure shows near-C_2 symmetry, with a flattened-tetrahedral four-coordinate structure around iron and a larger angle (133.80(9)°) between the two pyridyls, in contrast to the structure of Fe(L^0)$_2$ (where the corresponding angle is 106.5(2)°).[38] In Fe(HL)$_2$, the angle between the pyrrolides is small, 115.25(9)°, so that the (pyridyl)$_2$Fe angle can open and make room for the pendant pyrrole groups. These pyrroles direct their NH bonds *inward*, apparently to direct the bulky ^{t}Bu groups outward, toward the less crowded molecular surface. These two pendant rings have their planes approximately parallel (Figure 9), to minimize crowding, but the interatomic distances are all longer than 4.8 Å. These two pyrroles have dihedral angles toward their attached pyridyls of 41 and 57°, while the κ^2-coordinated

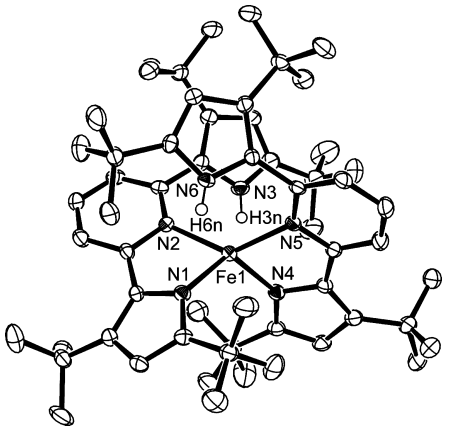

Figure 8. ORTEP view (50% probabilities) of the non-hydrogen atoms of Fe(HL)$_2$ viewed with the approximate C_2 axis vertical. Unlabeled atoms are carbon, and the two pyrrole NH hydrogens are shown. This shows the flattened-tetrahedral structure around iron and the inward direction of the NH hydrogens. Selected structural parameters (distances in Å and angles in deg): Fe1−N4, 2.011(2); Fe1−N1, 2.012(2); Fe1−N5, 2.055(2); Fe1−N2, 2.077(2); N4−Fe1−N1, 115.25(9); N4−Fe1−N5, 82.11(9); N1−Fe1−N2, 83.44(9); N5−Fe1−N2, 133.80(9).

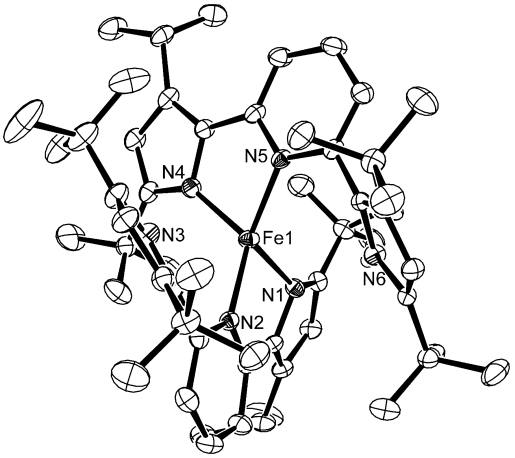

Figure 9. ORTEP view (50% probabilities) of Fe(HL)$_2$ viewed down the approximate C_2 axis, showing the face to face alignment of the two pyrroles bearing N3 and N6. Note also the misalignment of the N1 lone pair with respect to Fe1; Fe1 is not in the pyrrolide plane, involving N1. H on N3 is obscured by that nitrogen; H on N6 is visible.

pyridyl and pyrrolide have corresponding dihedral angles of 19 and 6°. Although the Fe−N(pyrrolide) distances are statistically identical, one of the pyrrolides (that with the 19° dihedral angle, containing N1) is significantly misdirected, not pointing its lone pair directly toward iron (Figure 9). This lack of bond lengthening with misdirected σ donation is unusual and, together with the large variations between angles in Fe(HL)$_2$ and Fe(L^0)$_2$, shows the coordination sphere of Fe(II) here to be highly deformable, or plastic. The distance between N1 and the proton on N6 is 2.613 Å, while that from the proton on N3 to N4 is 2.709 Å. Judging by the more reliably located nitrogens, the N6−N1 distance is 3.30 Å while the N3−N4 distance is 3.45 Å. The N6−H−N1 bond angle is 150° and so is in an acceptable range for hydrogen bonding. The N1 lone pair misdirection is also evident in the fact that the sum of angles around N1 is only 351.8° (i.e., nonplanar) while that around

dx.doi.org/10.1021/ic402120r | Inorg. Chem. 2014, 53, 1361−1369

N4 is 359.1°. This asymmetry of these hydrogen bonds degrades the C_2 symmetry slightly, but the Fe−N1 distance is not significantly longer than Fe−N4. This flexibility in the coordination sphere should translate into ready binding of a fifth ligand.

We felt that $Fe(HL)_2$, with its two NH functionalities, might have some potential for substrate transformation that exploited those hydrogens.[39−42] It is necessary to think more generally than merely H^+ transfer, and H atom transfer, perhaps as part of proton-coupled electron transfer, was anticipated. Another aspect of such reactivity would be that the nitrogen, once stripped of its hydrogen, is likely to coordinate to the metal, yielding an κ^3 pincer; such behavior might even promote release of the transformed substrate.

DISCUSSION AND CONCLUSIONS

At one point, we worried that the conformation of the free H_2L suggested that this ligand might favor κ^2 or (κ^1) binding to minimize ^{t}Bu clash with pyridyl ring atoms. Using complexes now in hand, distances between pyrrolide and pyridyl nitrogens can be used to evaluate the bite of this pincer. Of special interest is whether the ^{t}Bu groups ortho to the pyridyl ring create steric interference with the pyridyl ring hydrogens or whether that repulsion is beneficial by redirecting the pyrrolide nitrogens more inward, thus favoring smaller 3d transition metals. In fact, those N(pyridyl)−N(pyrrolide) nonbonded distances are 2.59−2.60 Å for *both* Pt(L)PhCN and (L)Zn-(DMAP). The similarity of the values for Pt and Zn suggests that the ligand does *not* strongly disfavor smaller metals. In every case, the ortho ^{t}Bu groups adopt a conformation which nests the tooth of the pyridyl meta CH in the gear of two ^{t}Bu methyls.

The size of the metal seems to influence the geometry of M(L)(Lewis base). The N(pyrrolide)−N(pyrrolide) distances are as follows: Pt, 4.058 Å; Zn, 3.825 Å. The smaller distance for Zn puts the ^{t}Bu groups closer to each other, eventually choking out any possible coordination of a base trans to the pyridyl ring and accounting for the unusual geometry of (L)Zn(DMAP) (see also Figure 6). This is equally evident from the distance between the two quaternary carbons on these ^{t}Bu groups: 6.83 Å for Pt and 6.22 Å for Zn.

The M−N(pyridyl) distance is shorter than the M−N(pyrr) distances by 0.11 Å in the Pt complex. The differences between M−N distances in the Fe and Zn complexes are less significant, and thus there are no generalizations possible about relative M−N distances involving these two ring types.

Two compounds characterized here, $Fe(HL)_2$ and (LH)-ZnEt, show that pendant monoprotonated pyrrole still permits the pincer ligand to be bidentate. This pendant pyrrole provides Brønsted acid functionality, or even two of these, nearby for useful subsequent reactivity.[43−45] Given the cyclization approach from β-diketones, the ligand is clearly modular: different substituents on the pyrrolide arms will open up a range of electronic/steric variants for ML complexes. In addition, the flexibility of the ligand in terms of mode of binding, bi- or tridentate and carrying a proton as HL^- or accepting a proton when it is L^{2-}, show the potential of this ligand class.

EXPERIMENTAL SECTION

General Procedures. All manipulations were carried out under an atmosphere of purified nitrogen using standard Schlenk techniques or in a glovebox. Solvents were purchased from commercial sources, purified either using an Innovative Technology SPS-400 PureSolv solvent system or distilling from conventional drying agents and degassing by the freeze−pump−thaw method twice prior to use or by activated alumina and Q-5 deoxygenation columns. Glassware was oven-dried at 150 °C overnight. NMR spectra were recorded in C_6D_6, THF-d_8, and toluene-d_8 at 25 °C or on a Varian Inova-400 spectrometer (^{1}H, 400.11 MHz; ^{13}C, 100.61 MHz; ^{19}F, 376.48 MHz) or on a 300 MHz spectrometer. Proton and carbon chemical shifts are reported in ppm versus Me_4Si. Electrochemical studies were carried out with an Autolab Model PGSTAT30 potentiostat (Eco Chemie). A three-electrode configuration consisting of a working electrode (platinum-button electrode), a $Ag/AgNO_3$ (0.01 M in MeCN with 0.1 M n-Bu_4NPF_6) reference electrode, and a platinum-coil counter electrode was used. All electrochemical potentials were referenced with respect to the Cp_2Fe/Cp_2Fe^+ redox couple, added internally with the sample at the end of a study.

Synthesis of 2,6-Bis(phthalimidomethyl)pyridine. The synthesis was carried out according to a literature method[46] with modifications. A mixture of 2,6-bis(hydroxymethyl)pyridine (4.9381 g, 35.49 mmol) and triphenylphosphine (18.7797 g, 71.60 mmol) was dissolved in THF (300 mL) and cooled to 0 °C. Phthalimide (10.8280 g, 73.60 mmol) was added, and diethyl azodicarboxylate ester (14.0 mL, 77.17 mmol) was subsequently added dropwise. The cooling bath was removed and the mixture was stirred for 1 day at room temperature. The solvent was evaporated, and the residue was washed with CH_2Cl_2 and dried under vacuum to give 2,6-bis-(phthalimidomethyl)pyridine (12.0225 g, 30.25 mmol, 85%) as a white powder. Without further purification, the product was used in the next step. ^{1}H NMR (400 MHz, $CDCl_3$): δ 4.89 (s, 4H) 7.10 (d, J = 7.6 Hz, 2H), 7.57 (t, J = 7.8 Hz, 1H), 7.66 (m, 4H), 7.73 (m, 4H).

Synthesis of 2,6-Bis(aminomethyl)pyridine. The synthesis was carried out according to some modification of a literature method.[46] Hydrazine hydrate (6 mL) was added to a solution of 2,6-bis(phthalimidomethyl)pyridine (4.9922 g, 12.56 mmol) in ethanol/water (120 mL/6 mL). The mixture was refluxed for about 30 min to form a white solid. After filtration and disposal of the solid, the solvent was evaporated from the filtrate on a rotary evaporator. After dissolution of the residue into $CHCl_3$ and filtration, the solvent was removed to give 2,6-bis(aminomethyl)pyridine (2.1242 g, 12.20 mmol, 97%) as a yellow oil. ^{1}H NMR (400 MHz, DMSO-d_6): δ 3.80 (s, 4H), 7.26 (d, J = 8.0 Hz, 2H), 7.70 (t, J = 7.8 Hz, 1H). ^{13}C NMR (101 MHz, DMSO-d_6): δ 52.57, 123.68, 141.92, 167.16.

Synthesis of 2,6-Bis(3,5-di-*tert*-butylpyrrol-2-yl)pyridine. Bis-(aminomethyl)pyridine (1.0 g, 7.3 mmol), 2,2,6,6-tetramethyl-3,5-heptadione (3.2 mL, 15.3 mmol,) and tosic acid hydrate (0.80 g, 4.7 mmol) were added to 250 mL of mesitylene in a three-neck flask equipped with a condenser and a Dean−Stark trap under nitrogen. The mixture was refluxed under N_2 for 4 days. After it was cooled, the crude material was passed through a column of silica to give a yellow solution. Upon removal of solvent, 1.29 g (41% yield) of 2,6-bis(3,5-di-*tert*-butylpyrrol-2-yl)pyridine was collected as a pale yellow solid. ^{1}H NMR (400 MHz, $CDCl_3$): δ 1.31 (s, 9H), 1.43 (s, 9H), 5.97 (d, J = 3.2 Hz, 2H), 7.35 (d, J = 8.0 Hz, 2H), 7.59 (t, J = 7.8 Hz, 1H), 8.86 (brs, 2H, *NH*). ^{13}C{^{1}H} NMR (101 MHz, $CDCl_3$): δ 30.5, 31.4, 31.5, 31.8, 104.5, 118.7, 124.9, 133.0, 135.6, 141.1, 151.9. GC-MS (EI): m/z 433 (M^+), 418 ($M^+ - CH_3$). If this reaction is done with a larger amount of tosic acid catalyst, the doubly amine protonated 2,6-bis(aminomethyl)pyridine ditosylate precipitates as a colorless salt (identified by ^{1}H NMR spectroscopy) and reduces the yield of the desired product.

Preparation of Potassium Salt of 2,6-Bis(3,5-di-*tert*-butyl-pyrrol-2-yl)pyridine. A 50.5 mg portion of 2,6-bis(3,5-di-*tert*-butylpyrrol-2-yl)pyridine (0.116 mmol) in 4 mL of THF was slowly added to a stirred mixture of 10.0 mg of KH (2.15 equiv, 0.249 mmol) in 4 mL of THF. After 2 h, the solution was filtered and used without further purification (removal of solvent yields a pale yellow solid). ^{1}H NMR (400 MHz, THF-d_8): δ 1.30 (s, 9H), 1.42 (s, 9H), 5.88 (s, 2H), 7.03 (d, J = 7.2 Hz, 2H), 7.21 (t, J = 7.8 Hz, 1H).

Synthesis of LPt(PhCN). Deprotonation of H_2L (90.6 mg, 0.209 mmol) with KH (25.3 mg, 0.631 mmol) in 13 mL of THF was carried

dx.doi.org/10.1021/ic402120r | Inorg. Chem. 2014, 53, 1361−1369

out with stirring for 2 h. After filtration through a Celite pad (Celite pad was then washed with 10 mL of THF), the solution was added to 109.5 mg (0.232 mmol) of $PtCl_2(NCPh)_2$ in 10 mL of THF at room temperature. The reaction mixture was stirred at room temperature for 1 h. After removal of solvent under vacuum, the residue was extracted with benzene. After filtration through Celite, the solvent was evaporated and the crude compound obtained. NMR analysis showed that the crude product was contaminated with free ligand. Recrystallization for toluene/pentane in −40 °C gave the pure platinum complex as a red powder. Yield: 28.5 mg (0.0390 mmol, 19%). ^{1}H NMR (400 MHz, C_6D_6): δ 1.20 (s, 9H), 1.68 (s, 9H), 6.28 (s, 2H), 6.61 (t, J = 7.3, 2H, Ph), 6.77 (t, J = 7.2, 1H, Ph), 6.85 (t, J = 7.8, 1H, py), 6.92 (d, J = 7.2, 2H, Ph), 6.96 (d, J = 7.8, 2H, py).

Synthesis of LPd(PhCN). Stirring 15.8 mg (0.394 mmol) of KH with 47.5 mg (0.110 mmol) of H_2L in 7 mL of THF yielded K_2L within 2 h. After filtration with a Celite pad (the Celite pad was washed with 5 mL of THF), the solution was added to 42.4 mg (0.111 mmol) of $PdCl_2(NCPh)_2$ in 3 mL of THF at room temperature. The reaction mixture was stirred at room temperature for 1 h. After removal of solvent under vacuum, the residue was extracted with benzene. The solid residue was recrystallized from toluene/hexane at −40 °C to give a red powder, yield 20.6 mg (0.321 mmol, 29%), following crystallization from toluene/hexane. ^{1}H NMR (400 MHz, C_6D_6): δ 1.33 (s, 9H), 1.56 (s, 9H), 6.46 (s, 2H), 6.63 (t, J = 7.3, 2H, Ph), 6.78 (t, J = 7.2, 1H, Ph), 6.87 (t, J = 7.8, 1H, py), 6.97 (d, J = 7.2, 2H, Ph), 7.08 (d, J = 7.8, 2H, py).

Carbonylation of LPd(NCPh). CD_2Cl_2 (0.5 mL) was vacuum-transferred in to an NMR tube (5 mm i.d. × 180 mm length) containing LPd(NCPh) (3.7 mg, 0.0058 mmol). The solution was degassed by freeze−pump−thaw cycles, and CO (0.1 MPa) was introduced. After the reaction mixture became dark, the sample tube was placed in an NMR probe and the ^{1}H NMR spectrum was measured. The ^{1}H NMR spectrum indicates formation of free PhCN and the palladium complex LPd(CO). ^{1}H NMR (CD_2Cl_2): δ 1.40 (s, 18H, tBu), 1.49 (s, 18H, tBu), 6.00 (s, 2H, pyrr), 7.06 (d, 2H, J = 8.0 Hz, py), 7.43 (t, 1H, J = 8.0 Hz, py). The IR spectrum in CH_2Cl_2 indicates formation of a carbonyl complex. IR (cm^{-1}, CH_2Cl_2): 2197 (ν_{CO}).

Synthesis of (HL)Zn(Et). Diethylzinc (0.1 mL of 1.0 M $ZnEt_2$ in diethyl ether, 0.1 mmol of $ZnEt_2$) was slowly added to a stirred solution of 34.3 mg of H_2L (0.079 mmol) in benzene at 25 °C. Upon mixing the solution turned bright yellow, and the reaction was complete after 30 min. Removal of solvent by vacuum gave a yellow powder: yield 36 mg (0.068 mmol, 86%). Crystals were grown by slow evaporation of a pentane solution. ^{1}H NMR (400 MHz, C_6D_6): δ 0.15 (q, J = 10.8 Hz, 2H, $-CH_2CH_3$), 1.15 (s, 9H), 1.23 (s, 9H), 1.31 (t, J = 10.8 Hz, 3H, $-CH_2CH_3$), 1.55 (s, 9H), 1.63 (s, 9H), 6.03 (d, $^4J_{H-NH}$ = 3.2 Hz, 1H, pyrrole), 6.51 (s, 1H, pyrrolide), 6.59 (d, J = 7.6 Hz, 1H, py), 6.95 (dd, J = 8.4, 7.6 Hz, 1H, py), 6.96 (br, 1H, NH), 7.81 (d, J = 8.4 Hz, 1H, py).

Synthesis of (HL)Zn(DMAP)(Et). A solution of *p*-dimethylaminopyridine (4.0 mg, 0.033 mmol) in C_6D_6 was slowly added to a stirred solution of (HL)Zn(Et) (17.9 mg, 0.034 mmol) in C_6D_6 at 25 °C. Upon mixing the solution became yellow green to form (HL)Zn(DMAP)(Et). Removal of solvent by vacuum gave a yellow-green powder. ^{1}H NMR (400 MHz, C_6D_6): δ 0.51 (q, J = 8.0 Hz, 2H, $-CH_2CH_3$), 1.24 (s, 9H), 1.25 (s, 9H), 1.60 (s, 9H), 1.69 (t, J = 8.0 Hz, 3H, $-CH_2CH_3$), 1.78 (s, 9H), 1.93 (s, 6H, Me), 5.68 (d, J = 5.6 Hz, 2H, DMAP), 6.15 (d, J = 3.2 Hz, 1H, pyrrole-H), 6.65 (s, 1H, pyrrolide-H), 6.74 (d, J = 7.6 Hz, 1H, py), 7.03 (apparent t, J = 8.0 Hz, 1H, py), 7.49 (br, 1H, NH), 7.75 (d, J = 5.6 Hz, 2H, DMAP), 7.99 (d, J = 8.4 Hz, 1H). In the presence of of a modest excess of DMAP, the DMAP lines broadened and those of the HL ligand changed chemical shift, consistent with the rapid exchange of free and coordinated DMAP on the NMR time scale.

Synthesis of Zn(L)(DMAP). (HL)Zn(DMAP)(Et) (65 mg, 0.10 mmol) was dissolved in 10 mL of C_6H_6 and gently heated to 50 °C for 20 min with stirring. When this solution was cooled to room temperature, the product Zn(L)(DMAP) precipitated as pale yellow needles. The product was filtered from the benzene solution and washed with benzene and pentane, and removal of solvent by vacuum gave solid Zn(L)(DMAP) in 86% yield (53 mg, 0.086 mmol). ^{1}H NMR (400 MHz, CD_2Cl_2): δ 1.39 (s, 18H, tBu), 1.45 (s, 18H, tBu), 2.95 (s, 6H, Me), 6.15 (s, 2H, pyrrolide-H), 6.37 (d, J = 6.8 Hz, 2H, DMAP), 6.99 (d, J = 6.8 Hz, 2H, DMAP), 7.17 (d, J = 8 Hz, 2H, py), 7.45 (t, J = 8 Hz, 1H, py). No decoalescence of peaks was observed down to −40 °C. All CV scans were done with Pt as the working electrode, Pt as the counter electrode, and Ag/AgCl wire as the reference electrode. $TBAPF_6$ (0.1 M) was employed as a supporting electrolyte. The solvent was *o*-difluorobenzene. A 10.1 mg portion of Zn complex was used. All CVs were referenced to internal Fc/Fc^+ as the standard, which appears at $E_{1/2}$ = +0.7115 V vs the reference electrode. The open circuit potential of Zn(L)(DMAP) was −0.460 V vs Fc/Fc^+.

Reaction of (HL)Zn(Et) with $LiN(SiMe_3)_2$. A solution of lithium bis(trimethylsilyl)amide (17.0 mg, 0.102 mmol) in C_6D_6 was slowly added to a stirred solution of (HL)Zn(Et) (50 mg, 0.095 mmol) in C_6D_6 at 25 °C. Upon mixing the solution became pale orange-yellow with formation of $NH(SiMe_3)_2$. The product solution contained unreacted (HL)Zn(Et) as well as a new pincer complex, assigned as [Zn(L)Et]Li. ^{1}H NMR (400 MHz, C_6D_6): δ 0.29 (s, $NH(SiMe_3)_2$), 0.37 (q, J = 10 Hz, 2H, CH_2CH_3), 0.97 (t, J = 10 Hz, 3H, CH_2CH_3) 1.23 (s, 18H, tBu), 1.52 (s, 18H, tBu), 6.23 (s, 2H, pyrrolide-H), 6.97 (t, overlaid by (HL)Zn(Et) peak, 1H, py), 7.29 (d, J = 7.6 Hz, 2H, py). After vacuum removal of volatiles, the ethyl peak disappeared, as well as most of the bis(trimethylsilyl)amine. What remained was a product containing a pincer ligand with equivalent pyrrolide arms, possibly [ZnL]Li or a dimer thereof. ^{1}H NMR (400 MHz, C_6D_6): δ 1.23 (s, 18H, tBu), 1.52 (s, 18H, tBu), 6.23 (s, 2H, pyrrolide-H), 6.97 (t, J = 8 Hz, 1H, py), 7.29 (d, J = 8 Hz, 2H, py).

Synthesis of $Fe(HL)_2$. KH (4.6 mg, 0.11 mmol) was added to a stirred solution of H_2L (50 mg, 0.11 mmol) in 10 mL of THF. After 30 min, the reaction was complete to form a 1:1 mixture of H_2L and K_2L in solution. A ^{1}H NMR spectrum in THF showed the persistence of H_2L in solution, as well as peaks which corresponded to K_2L, and these two species were present in a 1:1 ratio. No additional species were found in solution, suggesting that KHL is not a product of H_2L reacting with 1 equiv of KH. Solid $FeCl_2$ (7.3 mg, 0.058 mmol) was added to the stirred mixture and reacted for 2 h, forming a dark red solution. After removal of solvent under reduced pressure, the dark red product was extracted into pentane and KCl was filtered away. Upon removal of pentane $Fe(HL)_2$ (38 mg, 72% yield) remained as a dark red solid. ^{1}H NMR (400 MHz, C_6D_6): δ −56.44 (2H), −6.56 (bs, 18H, tBu), −1.74 (bs, 18H, tBu), 8.94 (bs, 18H, tBu), 13.56 (bs, 18H, tBu), 71.13 (2H), 78.70 (2H), 79.83 (2H). The two remaining proton resonances for the ligand backbone could not be located and are apparently hidden under other stronger resonances. Paramagnetism makes it difficult to use traditional features (line width or chemical shift) to assign which is the signal of the NH protons.

■ ASSOCIATED CONTENT

Ⓢ Supporting Information

Text and CIF files giving full crystallographic details and figures giving NMR spectra and CV scans. This material is available free of charge via the Internet at http://pubs.acs.org.

■ AUTHOR INFORMATION

Corresponding Author

*K.G.C.: e-mail, caulton@indiana.edu; tel, 812-855-4798.

Notes

The authors declare no competing financial interest.

■ ACKNOWLEDGMENTS

We thank Indiana University Bloomington (FRSP) for financial support of this research. N.K. acknowledges support from JSPS Institutional Program for Young Researcher Overseas Visits.

We thank Atanu K. Das for crystal growth skills and Keith Searles for CV measurements.

REFERENCES

(1) Morales-Morales, D.; Jensen, C. M. *The Chemistry of Pincer Compounds*; 1st ed.; Oxford Elsevier: Amsterdam, 2007.
(2) Chirik, P. J.; Wieghardt, K. *Science* **2010**, *327*, 794.
(3) Fryzuk, M. D.; Montgomery, C. D. *Coord. Chem. Rev.* **1989**, *95*, 1.
(4) Hawk, J. L.; Craig, S. L. *Top. Organomet. Chem.* **2013**, *40*, 319.
(5) Limberg, C. *Angew. Chem., Int. Ed.* **2009**, *48*, 2270.
(6) Lyaskovskyy, V.; de Bruin, B. *ACS Catal.* **2012**, *2*, 270.
(7) Slagt, M. Q.; van Zwieten, D. A. P.; Moerkerk, A. J. C. M.; Gebbink, R. J. M. K.; van Koten, G. *Coord. Chem. Rev.* **2004**, *248*, 2275.
(8) van der Boom Milko, E.; Milstein, D. *Chem. Rev.* **2003**, *103*, 1759.
(9) van Koten, G. *J. Organomet. Chem.* **2013**, *730*, 156.
(10) Vigalok, A.; Milstein, D. *Acc. Chem. Res.* **2001**, *34*, 798.
(11) Flores, J. A.; Andino, J. G.; Tsvetkov, N. P.; Pink, M.; Wolfe, R. J.; Head, A. R.; Lichtenberger, D. L.; Massa, J. P.; Caulton, K. G. *Inorg. Chem.* **2011**, *50*, 8121.
(12) Flores, J. A.; Komine, N.; Pal, K.; Pinter, B.; Pink, M.; Chen, C.-H.; Caulton, K. G.; Mindiola, D. J. *ACS Catal.* **2012**, *2*, 2066.
(13) Searles, K.; Pink, M.; Caulton, K. G.; Mindiola, D. J. *Dalton Trans.* **2012**, *41*, 9619.
(14) Franceschi, F.; Guillemot, G.; Solari, E.; Floriani, C.; Re, N.; Birkedal, H.; Pattison, P. *Chemistry* **2001**, *7*, 1468.
(15) Korobkov, I.; Gambarotta, S.; Yap, G. P. A. *Organometallics* **2001**, *20*, 2552.
(16) Korobkov, I.; Vidjayacoumar, B.; Gorelsky, S. I.; Billone, P.; Gambarotta, S. *Organometallics* **2010**, *29*, 692.
(17) Solari, E.; Crescenzi, R.; Jacoby, D.; Floriani, C.; Chiesi-Villa, A.; Rizzoli, C. *Organometallics* **1996**, *15*, 2685.
(18) Yunlu, K.; Basolo, F.; Rheingold, A. L. *J. Organomet. Chem.* **1987**, *330*, 221.
(19) Liu, Q.; Thorne, L.; Kozin, I.; Song, D.; Seward, C.; D'Iorio, M.; Tao, Y.; Wang, S. *Dalton Trans.* **2002**, 3234.
(20) Jia, W.-L.; Liu, Q.-D.; Wang, R.; Wang, S. *Organometallics* **2003**, *22*, 4070.
(21) Klappa, J. J.; Rich, A. E.; McNeill, K. *Org. Lett.* **2002**, *4*, 435.
(22) Oxidation at the metal would be more difficult for Pd than for Pt, in contrast to the observations here.
(23) Irving, R. J.; Magnusson, E. A. *J. Chem. Soc.* **1958**, 2283.
(24) Bollermann, T.; Gemel, C.; Fischer, R. A. *Coord. Chem. Rev.* **2012**, *256*, 537.
(25) Campbell, W. M.; Burrell, A. K.; Officer, D. L.; Jolley, K. W. *Coord. Chem. Rev.* **2004**, *248*, 1363.
(26) Li, L.-L.; Diau, E. W.-G. *Chem. Soc. Rev.* **2013**, *42*, 291.
(27) Mangani, S.; Carloni, P.; Orioli, P. *Coord. Chem. Rev.* **1992**, *120*, 309.
(28) Spielmann, J.; Piesik, D.; Wittkamp, B.; Jansen, G.; Harder, S. *Chem. Commun.* **2009**, 3455.
(29) Vahrenkamp, H. *Dalton Trans.* **2007**, 4751.
(30) Anantharaman, G.; Chandrasekhar, V.; Nehete, U. N.; Roesky, H. W.; Vidovic, D.; Magull, J. *Organometallics* **2004**, *23*, 2251.
(31) Anantharaman, G.; Roesky, H. W.; Schmidt, H.-G.; Noltemeyer, M.; Pinkas, J. *Inorg. Chem.* **2003**, *42*, 970.
(32) Storre, J.; Schnitter, C.; Roesky, H. W.; Schmidt, H.-G.; Noltemeyer, M.; Fleischer, R.; Stalke, D. *J. Am. Chem. Soc.* **1997**, *119*, 7505.
(33) Roesky, H. W.; Walawalkar, M. G.; Murugavel, R. *Acc. Chem. Res.* **2001**, *34*, 201.
(34) Roesky, H. W.; Murugavel, R.; Walawalkar, M. G. *Chem. Eur. J.* **2004**, *10*, 324.
(35) Roesky, H. W.; Singh, S.; Jancik, V.; Chandrasekhar, V. *Acc. Chem. Res.* **2004**, *37*, 969.
(36) Hao, H.; Bhandari, S.; Ding, Y.; Roesky, H. W.; Magull, J.; Schmidt, H.-G.; Noltemeyer, M.; Cui, C. *Eur. J. Inorg. Chem.* **2002**, *5*, 1060.
(37) Caulton, K. G. *New J. Chem.* **1994**, *18*, 25.
(38) Searles, K.; Das, A. K.; Buell, R. W.; Pink, M.; Chen, C.-H.; Pal, K.; Morgan, D. G.; Mindiola, D. J.; Caulton, K. G. *Inorg. Chem.* **2013**, *52*, 5611.
(39) Clapham, S. E.; Hadzovic, A.; Morris, R. H. *Coord. Chem. Rev.* **2004**, *248*, 2201.
(40) Fong, H.; Moret, M.-E.; Lee, Y.; Peters, J. C. *Organometallics* **2013**, *32*, 3053.
(41) Grotjahn, D. B. *Top. Catal.* **2010**, *53*, 1009.
(42) Noyori, R.; Koizumi, M.; Ishii, D.; Ohkuma, T. *Pure Appl. Chem.* **2001**, *73*, 227.
(43) Ikariya, T. *Bull. Chem. Soc. Jpn.* **2011**, *84*, 1.
(44) Umehara, K.; Kuwata, S.; Ikariya, T. *J. Am. Chem. Soc.* **2013**, *135*, 6754.
(45) Watanabe, M.; Kashiwame, Y.; Kuwata, S.; Ikariya, T. *Chem. Lett.* **2010**, *39*, 758.
(46) Schohe-Loop, R.; Seidel, P.-r.; Bullock, W.; Feurer, A.; Terstappen, G.; Schuhmacher, J.; Vander Staay, F.-j.; Schmidt, B.; Fanelli, R. J.; Chisholm, J. C.; McCarthy, R. T. US Patent 5756517, 1998.